

In silico screening and computational evaluation of novel promising USP14 inhibitors targeting the palm-thumb pocket

Tianhao Wang^{1,2}, Jianbo Tong^{1*}, Xing Zhang^{1,2}, Hao Luo², Lei Xu³, Zhe Wang^{2*}

¹College of Chemistry and Chemical Engineering, Shaanxi University of Science and Technology, Xi'an 710021, P. R. China

²Innovation Institute for Artificial Intelligence in Medicine of Zhejiang University, College of Pharmaceutical Sciences, Zhejiang University, Hangzhou 310058, Zhejiang, P. R. China

³Institute of Bioinformatics and Medical Engineering, School of Electrical and Information Engineering, Jiangsu University of Technology, Changzhou 213001, China

Corresponding authors:

Jianbo Tong

E-mail: jianbotong@aliyun.com

Zhe Wang

E-mail: wangzhehyd@zju.edu.cn

Table S1. Cross Prime MM-GBSA re-scoring of inhibitors with crystal structures

Protein	Ligand			
	IU1	IU1-47	IU1-206	IU1-248
6HK	-61.45	-52.29	-51.37	-48.68
6IL	-58.00	-51.29	-49.64	-54.72
6IM	-60.08	-50.66	-51.62	-46.18
6IN	-56.67	-55.34	-63.39	-52.83

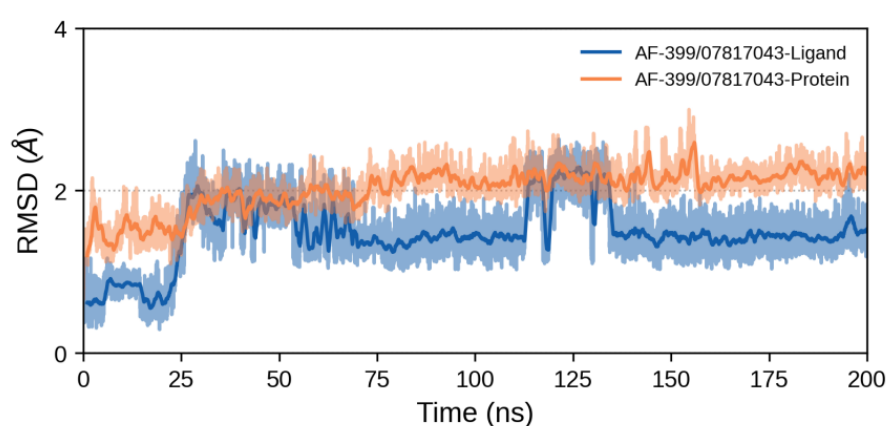


Figure S1. RMSD of the complex of ligand AF-399/07817043 and 6IL throughout the time of MD simulations

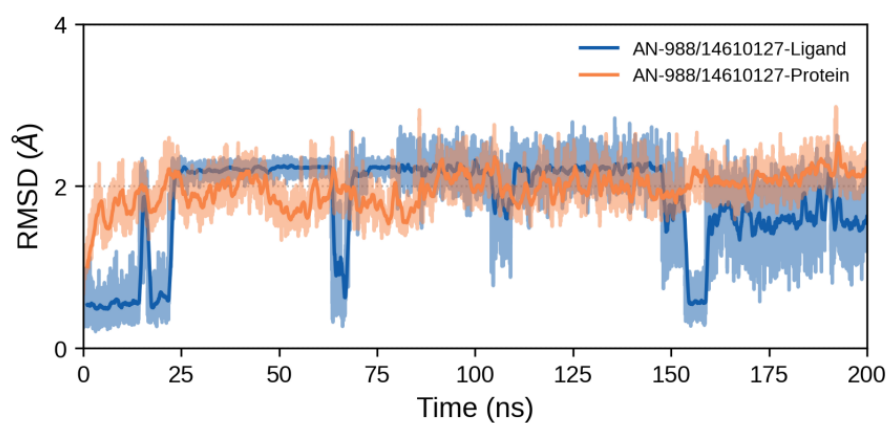


Figure S2. RMSD of the complex of ligand AN-988/14610127 and 6IL throughout the time of MD simulations

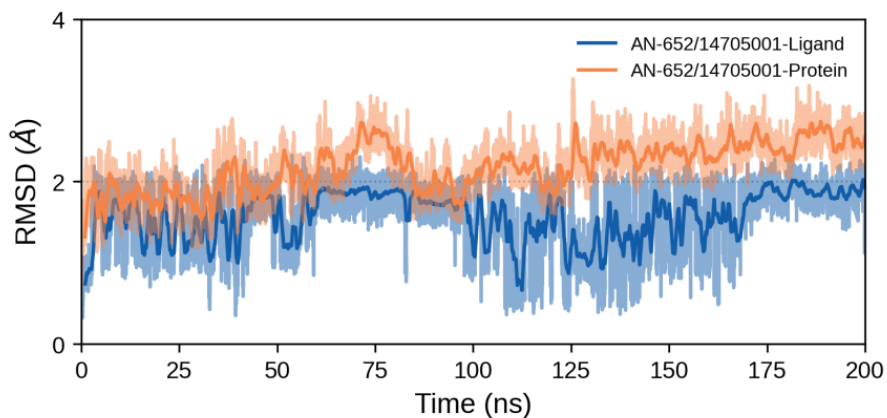


Figure S3. RMSD of the complex of ligand AN-652/14705001 and 6IIL throughout the time of MD simulations

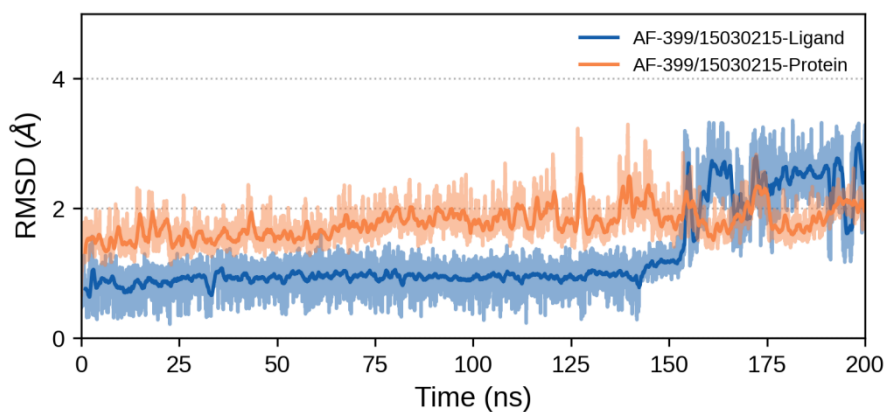


Figure S4. RMSD of the complex of ligand AF-399/15030215 and 6IIL throughout the time of MD simulations

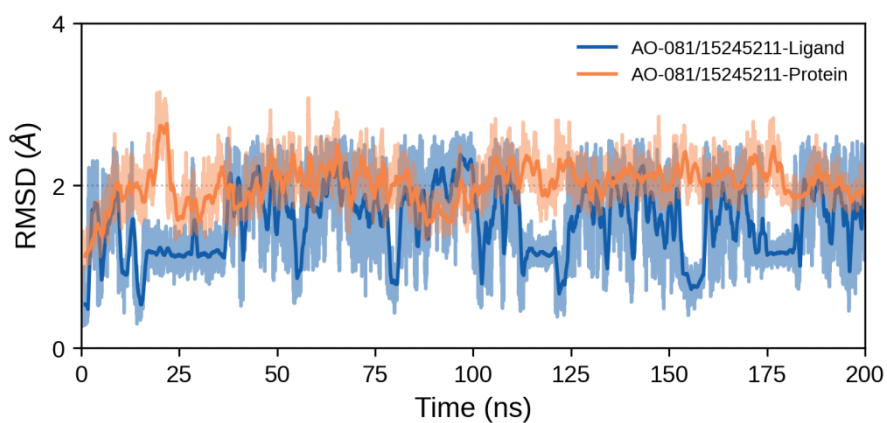


Figure S5. RMSD of the complex of ligand AO-081/15245211 and 6IIL throughout the time of MD simulations

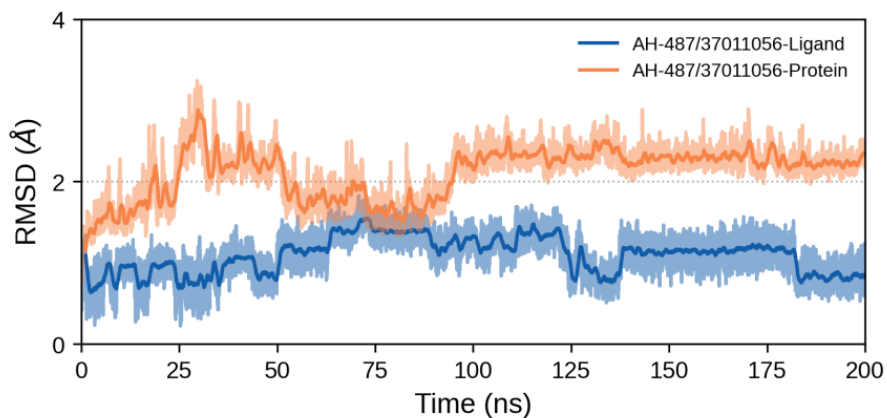


Figure S6. RMSD of the complex of ligand AH-487/37011056 and 6IIL throughout the time of MD simulations

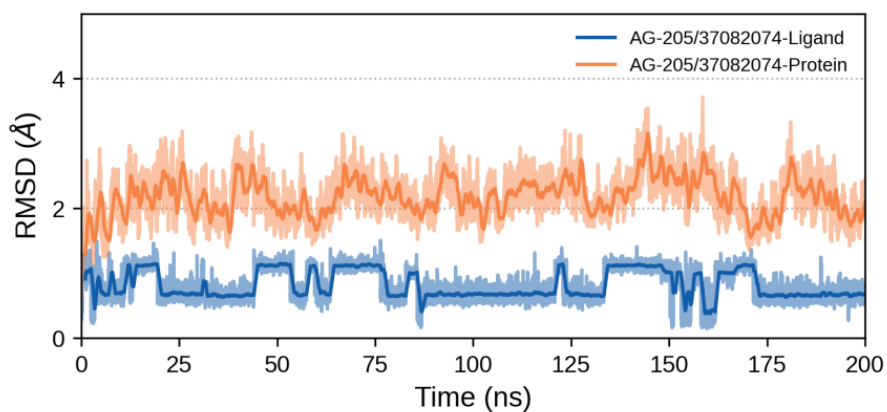


Figure S7. RMSD of the complex of ligand AG-205/37082074 and 6IIL throughout the time of MD simulations

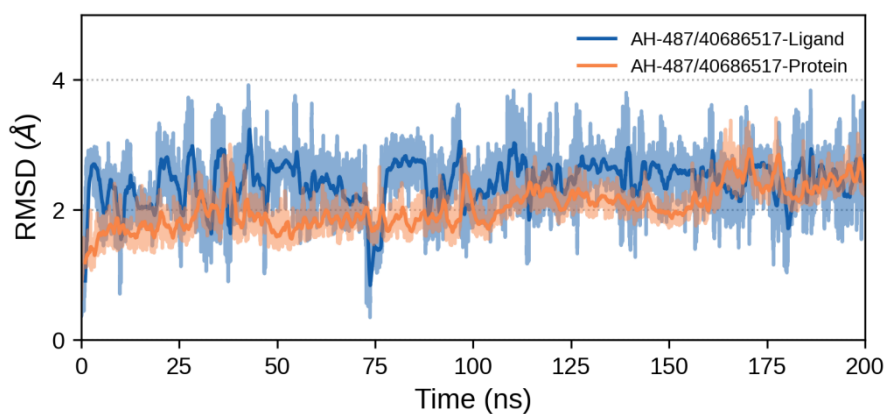


Figure S8. RMSD of the complex of ligand AH-487/40686517 and 6IIL throughout the time of MD simulations

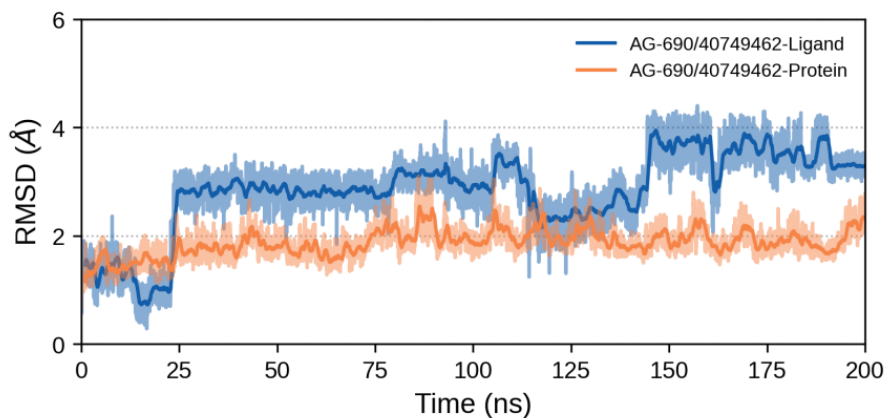


Figure S9. RMSD of the complex of ligand AG-690/40749462 and 6IIL throughout the time of MD simulations

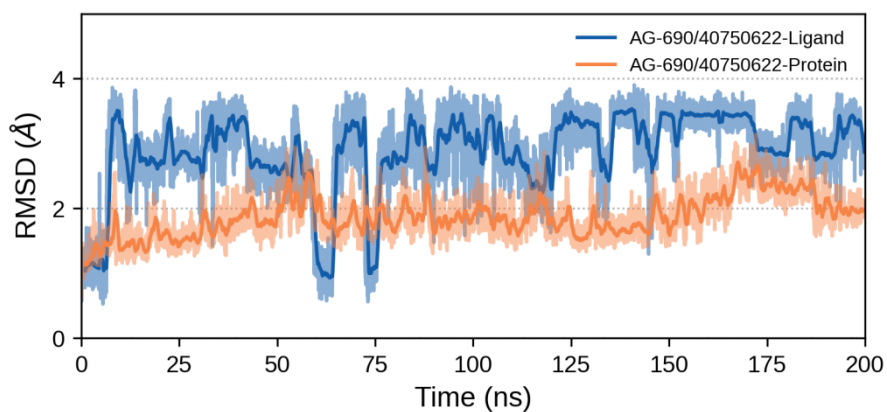


Figure S10. RMSD of the complex of ligand AG-690/40750622 and 6IIL throughout the time of MD simulations

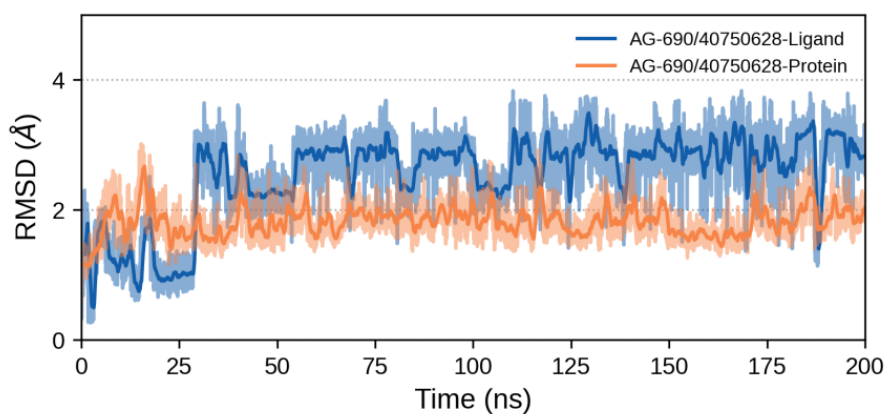


Figure S11. RMSD of the complex of ligand AG-690/40750628 and 6IIL throughout the time of MD simulations

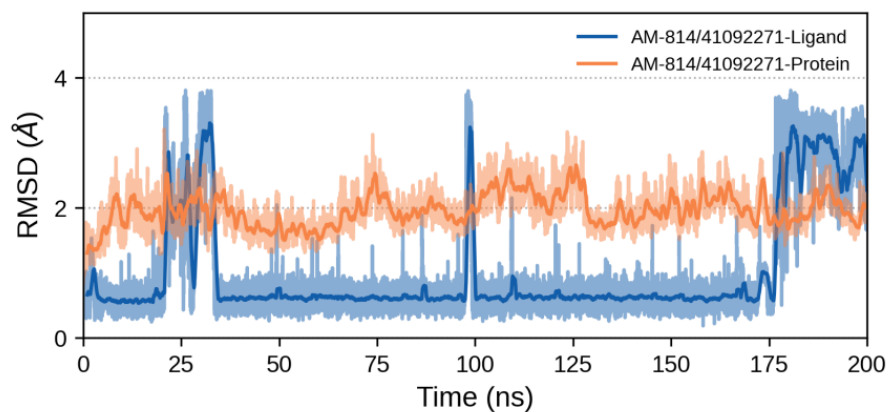


Figure S12. RMSD of the complex of ligand AM-814/41092271 and 6IIL throughout the time of MD simulations

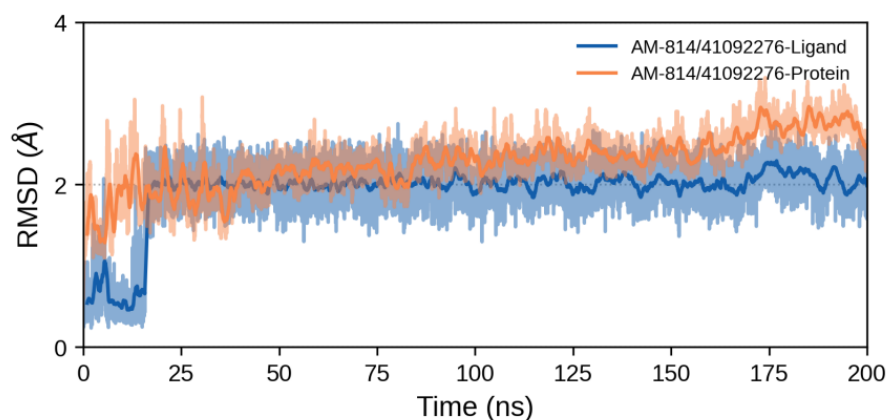


Figure S13. RMSD of the complex of ligand AM-814/41092276 and 6IIL throughout the time of MD simulations

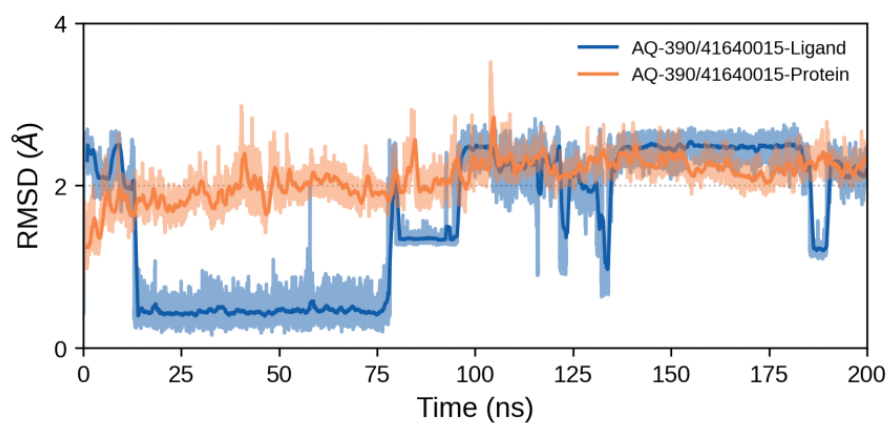


Figure S14. RMSD of the complex of ligand AQ-390/41640015 and 6IIL throughout the time of MD simulations

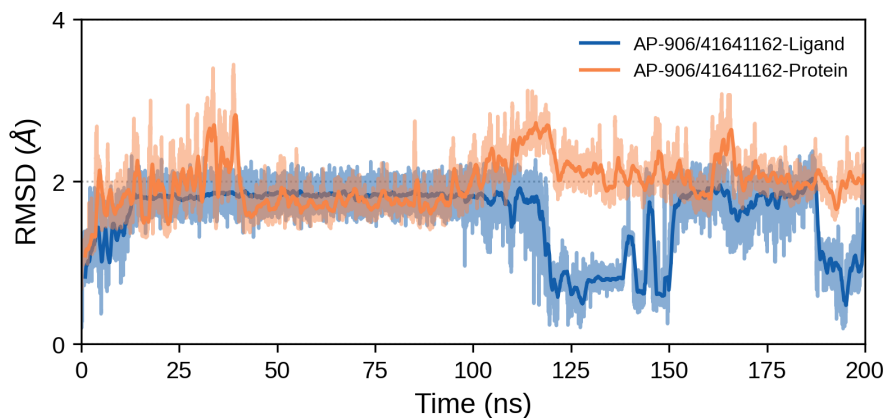


Figure S15. RMSD of the complex of ligand AP-906/41641162 and 6IIL throughout the time of MD simulations

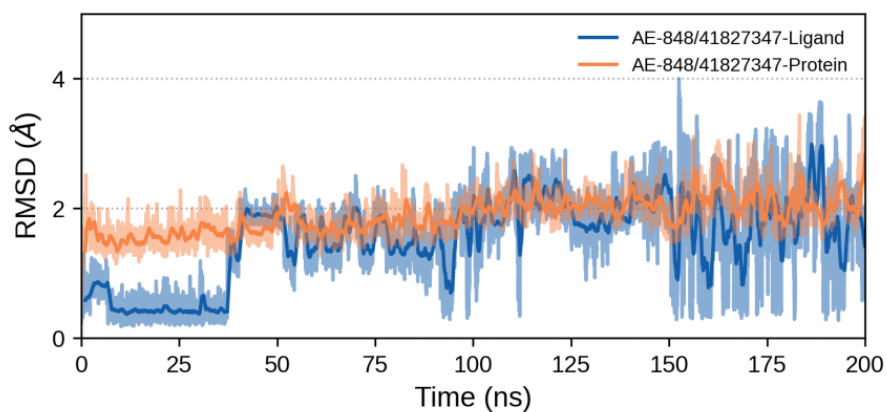


Figure S16. RMSD of the complex of ligand AE-848/41827347 and 6IIL throughout the time of MD simulations

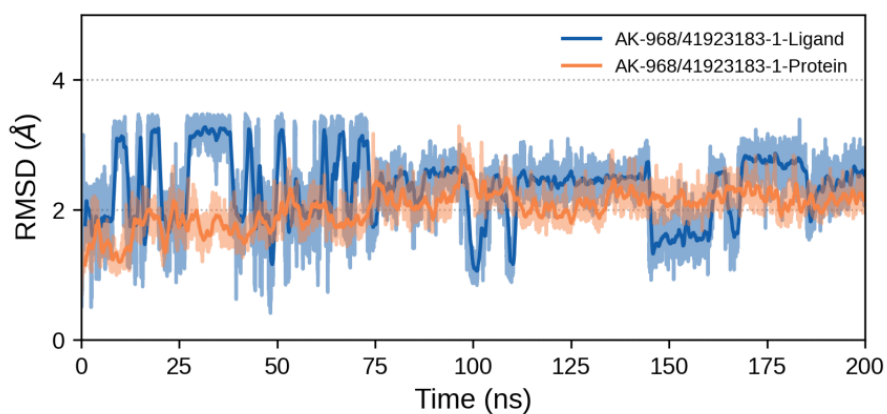


Figure S17. RMSD of the complex of ligand AK-968/41923183-1 and 6IIL throughout the time of MD simulations

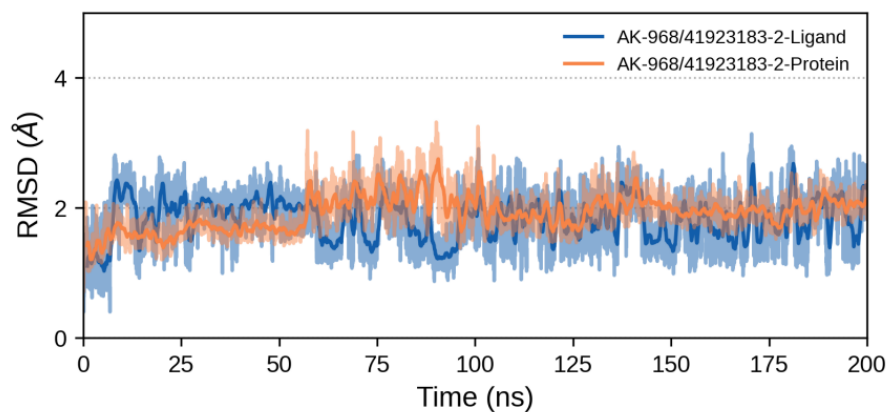


Figure S18. RMSD of the complex of ligand AK-968/41923183-2 and 6IIL throughout the time of MD simulations

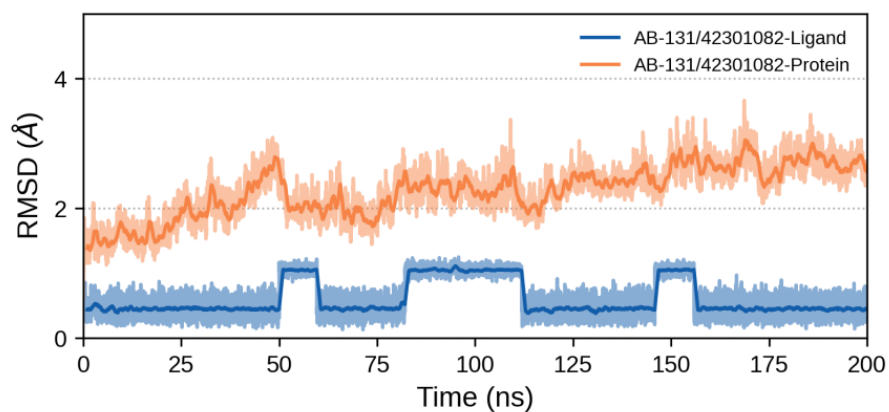


Figure S19. RMSD of the complex of ligand AB-131/42301082 and 6IIL throughout the time of MD simulations

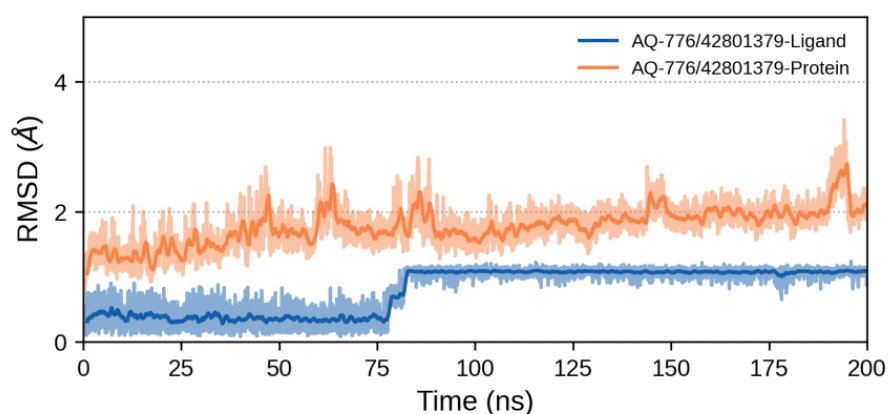


Figure S20. RMSD of the complex of ligand AQ-776/42801379 and 6IIL throughout the time of MD simulations

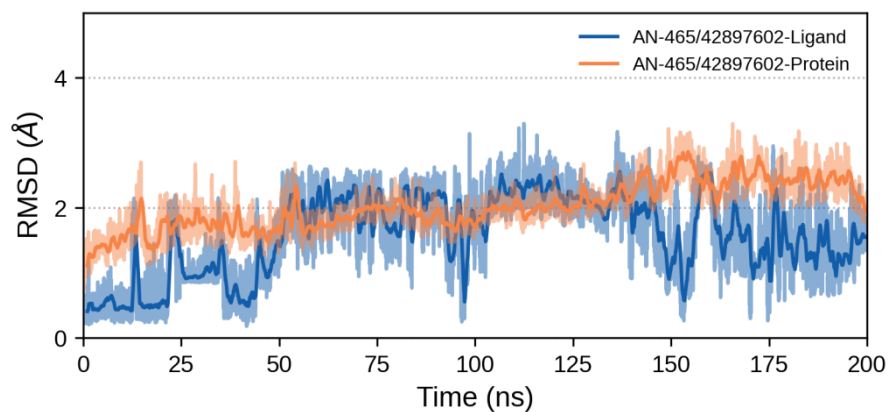


Figure S21. RMSD of the complex of ligand AN-465/42897602 and 6IIL throughout the time of MD simulations

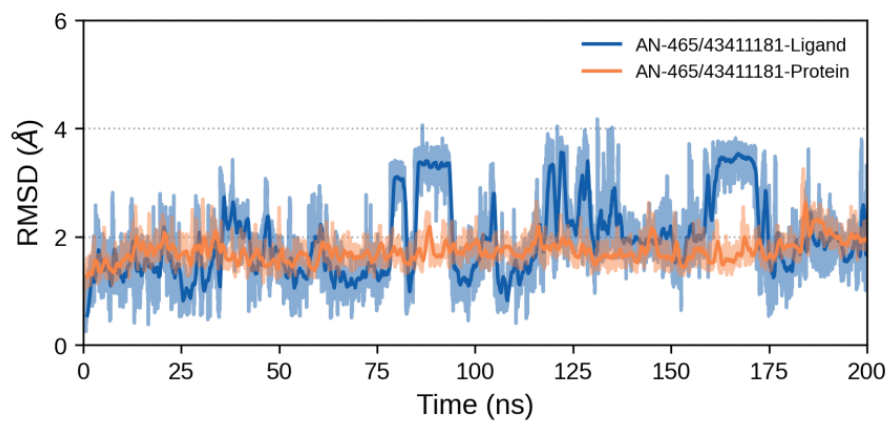


Figure S22. RMSD of the complex of ligand AN-465/43411181 and 6IIL throughout the time of MD simulations

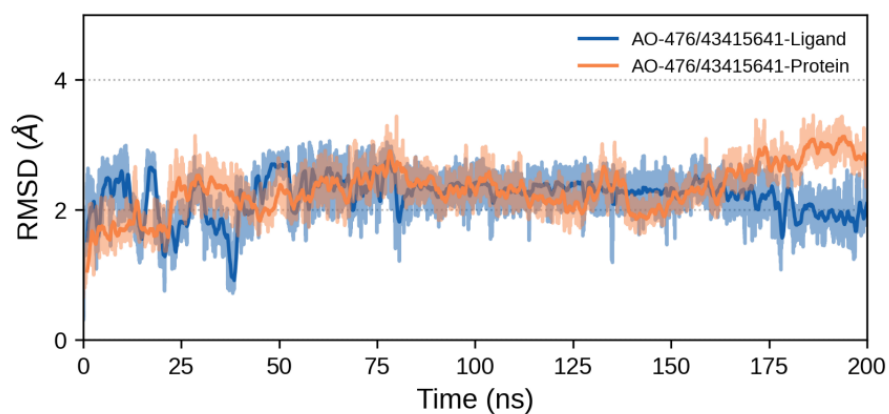


Figure S23. RMSD of the complex of ligand AO-476/43415641 and 6IIL throughout the time of MD simulations

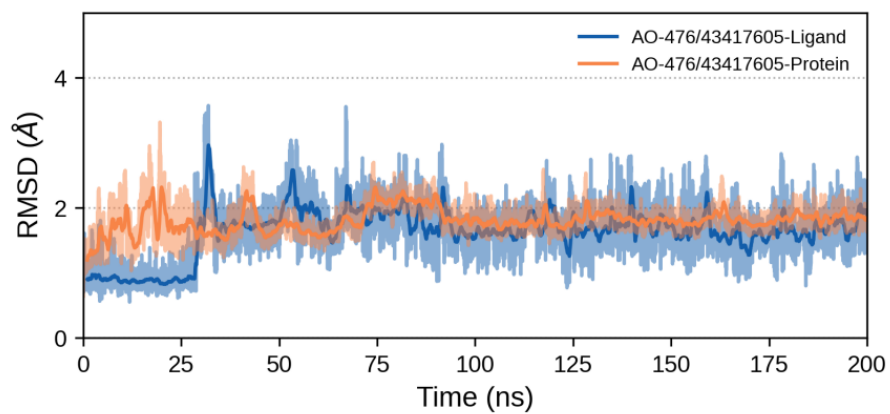


Figure S24. RMSD of the complex of ligand AO-476/43417605 and 6IIL throughout the time of MD simulations